ORGANOMETALLICS

Article

pubs.acs.org/Organometallics

Mechanistic Insights of a Concerted Metalation−Deprotonation Reaction with $[Cp^*RhCl_2]_2$

Aaron P. Walsh and William D. Jones*

Department of Chemistry, University of Rochester, Rochester, New York 14627, United States

Supporting Information

ABSTRACT: The effect of the carboxylate used in a concerted metalation−deprotonation reaction is probed and shows a direct correlation of pK_a to observed rate up to a pK_a of 4.3, where the rate drops off at higher pK_a. The rate of the C−H activation of 2-(4-methoxyphenyl)pyridine with $[Cp^*RhCl_2]_2$ and carboxylate follows first-order kinetics in the active metal species, $Cp^*RhCl(\kappa^2\text{-OAc})$, and zero-order kinetics in substrate when in a 1:1 ratio. There is a first-order dependence on substrate observed when excess substrate is present. The evaluation of the mechanism using kinetic studies allowed for a mechanistic proposal in which a second Ph′Py coordinates prior to the rate-determining C−H activation.

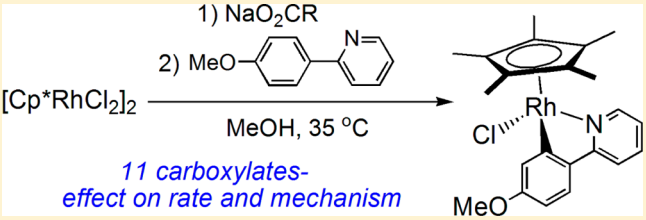

INTRODUCTION

C−H activation is a practical and efficient process by which unactivated hydrocarbons can be converted into functionalized materials. The lack of requirement of a preactivated compound provides a method where potentially hazardous waste and byproducts can be reduced or eliminated, which makes for a powerful tool in the synthesis of organic molecules. C−H bonds are ubiquitous but typically unreactive.[1] The cleavage of a C−H bond, in place of the more commonly used carbon−halogen bond, still requires the use of a highly reactive, oftentimes low-valent, metal fragment. A large excess of substrate is usually used to overcome the activation barrier, which can also reduce selectivity.[2]

Heteroatom directing groups offer the advantage of providing selectivity and the use of milder conditions.[3] Nitrogen-containing directing groups, specifically nitrogen-based heterocycles, are advantageous because of their favorable, yet reversible, coordination to metal complexes and their prevalence in medicinally relevant compounds.[4] A fundamental understanding of the mechanism by which C−H activation occurs, leading to cyclometalated products, is key to further development of these processes to become more applicable.[5] While there are several mechanistically feasible pathways for C−H activation to occur, two stand out: the classic oxidative addition, where an electron-rich metal species inserts into a C−H bond, and concerted metalation−deprotonation (CMD), where an electrophilic metal species simultaneously replaces a C−H bond with a carbon−metal bond with the assistance of a Lewis base such as carboxylate.[6] Systems based on the CMD pathway have been recently exploited by Fagnou,[7] Ellman,[8], and Ackermann,[3d,9] displaying reactivity with different metals. Pfeffer developed functionalizations of this type with Pd(II) over 20 years ago,[10] before the CMD reaction classification had been coined. The Fagnou group developed an innovative "redox-neutral" C−H bond functionalization with Rh(III) by the use of a built-in oxidant. They described the first example of Rh(III)-catalyzed synthesis of isoquinolones by electrophilic directed ortho-C−H alkenylation of *N*-methoxybenzamide, which subsequently forms a C−N bond. The cleavage of the N−O bond facilitates the regeneration of the Rh(III) catalyst and release of the product (eq 1).[7c]

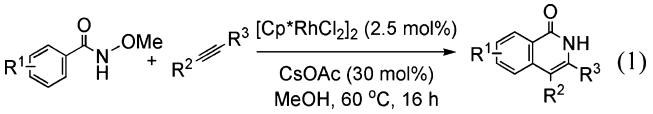

(1)

Ellman and Bergman have successfully developed an electrophilic rhodium-catalyzed synthesis of branched amines via C−H functionalization of benzamides with *N*-sulfonyl aldimines.[8c] The prospect of medicinal relevance with benzamides, the mild conditions of the protocol, and good functional group compatibility provide a powerful tool to rapidly access these motifs. The Ellman group had previously shown the proof of concept by adding *N*-Boc- and *N*-sulfonyl imines to 2-arylpyridine C−H bonds laying the groundwork, although pyridine moieties in biologically attractive targets are of limited use.[8b] Recently the Ellman group has used these precedents to develop the first reported asymmetric variant of intermolecular imine addition to nonacidic C−H bonds of benzamides that proceed in a diastereomeric ratio of at least 98:2 (eq 2).[8d]

Ruthenium can also be employed as an effective directed electrophilic C−H activation catalyst which has the benefit of being lower cost than similar rhodium-based catalysts. The Ackermann group has provided significant contributions to the area of electrophilic C−H activation via the concerted metalation−deprotonation mechanism using ruthenium cata-

Received: May 4, 2015
Published: July 1, 2015

DOI: 10.1021/acs.organomet.5b00369
Organometallics 2015, 34, 3400−3407

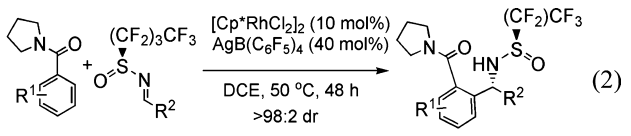

(2)

lysts. Specifically, they have looked at the carboxylate ion as a cocatalyst instead of as a stoichiometric additive. By investigation of the aptitude of several bulky carboxylates as effective assistants in direct regioselective arylations, aryl bromides, and in some cases even aryl chlorides, gave excellent yields (Scheme 1).[9b]

Scheme 1. Aptitude of Carboxylates As Cocatalysts for Directed C−H Arylation[a]

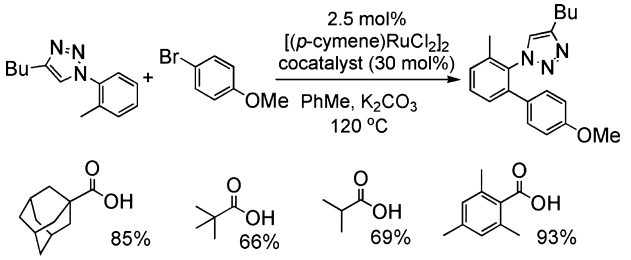

[a]Yields are for isolated product.

Mechanistic work has been done in some cases.[7,8d,9c] These studies have been largely performed by the Davies group[11] and our group.[12] Seminal work from Davies and co-workers[11f,g] led them to propose that the active species for electrophilic C−H activation is CpIr(κ^2-OAc)$^+$ using DFT calculations. The cation would bind *N*,*N*-dimethylbenzylamine (DMBA-H), and conversion of CpIr$^+$(κ^2-OAc)(DMBA-H) to CpIr$^+$(κ^2-C,N-DMBA)(η^1-O=C(OH)Me) occurred via a single, six-membered transition state (E = +16.0 kcal/mol) where the proximal acetate oxygen is displaced by the incoming C−H bond. This leads directly to insertion of iridium into the C−H bond with the hydrogen being transferred to the acetate. The product is lower in energy than the CpIr$^+$(κ^2-OAc)(DMBA-H) precursor (E = −2.4 kcal/mol). Davies also made a comparison to other feasible pathways (Figure 1). If oxidative addition were to occur

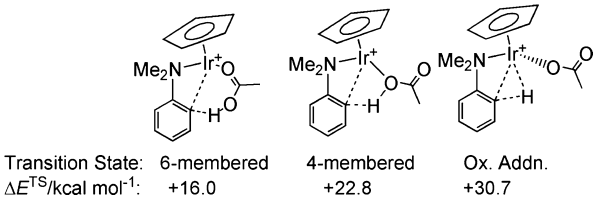

Figure 1. Calculated transition states for acetate-assisted C−H activation with {CpIr$^+$}.

at iridium with the acetate acting as a proton acceptor, the transition state found by DFT would be almost twice as high in energy (E = +30.7 kcal/mol).[11e]

The Davies group has also looked at the aptitude of four other carboxylates, RCO_2 (where R = CCl_3, CF_3 Ph, OH), with iridium and found that the C−H activation barrier was directly correlated to the ability of the intermediate [CpIr(κ^2-CO_2R)(DMBA-H)]$^+$ to generate an open site. They found that the weaker the coordinating ability of the carboxylate, the lower the barrier for C−H activation. The cleavage of the C−H bond reflected the pK_a of the carboxylate in that a more favorable C−H cleavage (thermodynamically) was associated with a less favorable κ^2−κ^1 displacement.[11d]

The work we have performed on the acetate-assisted C−H activation of phenyl imines and phenylpyridines with [Cp*MCl_2]$_2$ (M = Ir, Rh) probed the regioselectivity using a series of meta-substituted phenyl imines (−CF_3, −CN, −F, −COOMe, −CH_3, and −OMe) and 2-phenylpyridines (−CF_3, −CH_3, and −OMe).[12] These studies found that C−H activation was very sensitive to steric encumbrance, leading only to the meta-substituted product in several cases. Furthermore, substrates with electron-donating substituents reacted more quickly than substrates with electron-withdrawing substituents, which is attributed to the electrophilic nature of the C−H activation. The kinetics of these reactions were also studied. It was found that reactions with iridium were faster than those with rhodium and the rates fit second-order kinetics (first order in [Rh]; first order in [imine]) in most cases examined. The study herein describes the effect of pK_a of the carboxylate additive on the cyclometalation of 2-(4-methoxyphenylpyridine) (Ph′Py) and the observed kinetics of the system as a function of concentration.

RESULTS AND DISCUSSION

Synthesis and Characterization of Cp*RhCl(2-(4-methoxyphenyl)pyridine). Cp*RhCl(2-(4-methoxyphenyl)-pyridine) was synthesized using the protocol developed previously to yield metallacycle **4** in good yield (Scheme 2).[13] Single-crystal X-ray structure determination was achieved

Scheme 2. In Situ Formation of Active Rh^{III} Species in a Reaction with Ph′Py

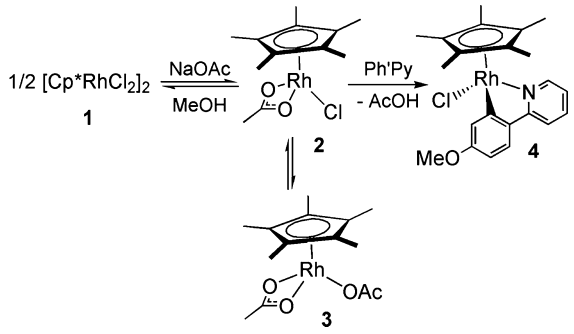

for complex **4**, and it was found to be isostructural with similar rhodium-containing metallacycles with *o*- and *m*-methoxy substituted phenylpyridines (Figure 2). Characterization by UV−vis spectroscopy showed a single shoulder in the spectrum at 338 nm (ε = 10005 L mol^{-1} cm^{-1}), and a linear Beer's law plot is shown in the Supporting Information.

This system was selected for further study due to the convenience of kinetic measurement of the rhodium complex in comparison to that of iridium. In comparison to our previous work with benzylideneanilines, the use of the more electron-rich 2-(4-methoxyphenyl)pyridine rather than 2-phenylpyridine led to appreciably faster reaction rates. We also found that following these reactions by UV−vis proved more reliable and convenient than using NMR spectroscopy (vide infra). All reactions could be performed on the bench with no exclusion of air and using reagent grade methanol that had not been dried, as there was no appreciable effect upon the observed reaction

DOI: 10.1021/acs.organomet.5b00369
Organometallics 2015, 34, 3400−3407

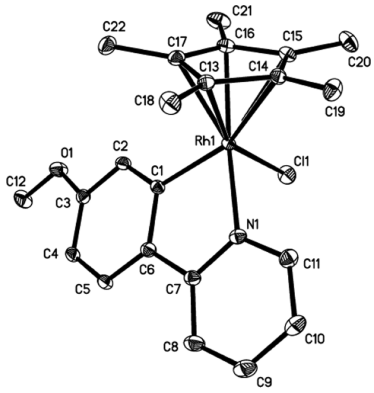

Figure 2. Molecular structure and atom-numbering scheme of **4** with 50% displacement ellipsoids. H atoms have been omitted for clarity.

rate when using methanol that had been dried over 4 Å molecular sieves.

Reaction Kinetics. The reaction shown in eq 3 was examined under stoichiometric conditions with 1 equiv of Ph′Py per rhodium and 1.5 equiv of carboxylate per rhodium. All of the reactions follow first-order kinetics in rhodium and zero-order kinetics in Ph′Py: i.e., product formation follows eq 4 with R^2 values of 0.995−0.999. Figure 3 shows the progress of

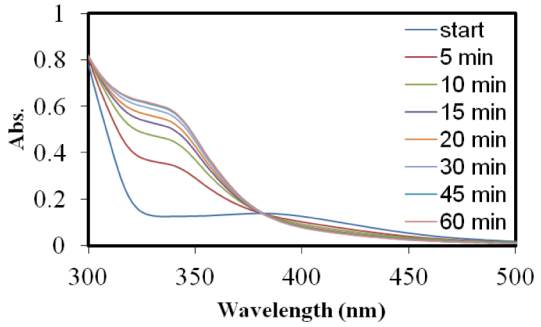

Figure 3. Observation of product formation over time via UV−vis. Conditions: [Rh] = [Ph′Py] = 0.627 mM; [NaOAc] = 0.934 mM; in MeOH at 35 °C.

the reaction described in eq 3 with sodium acetate, showing a clean isosbestic point for the conversion of **1** into **4**. Figure 5 shows the progress of the reactions with 11 different carboxylates. The observation of first-order kinetics in what appears to be a bimolecular reaction can be accommodated by quantitative formation of an adduct of the rhodium with the phenylpyridine. Low-temperature NMR experiments show evidence for the formation of such an adduct (Figures S5 and S6 in the Supporting Information).

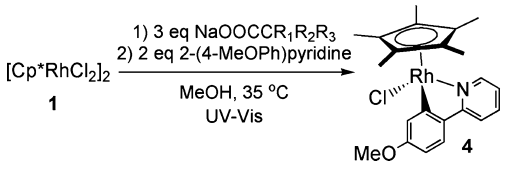

(3)

$$[\mathbf{4}] = [C_0 - C_I](1 - e^{-k_{obs}t}) + C_i \quad (4)$$

The slight excess of carboxylate salt added is necessary to keep the equilibrium of $[Cp^*RhCl_2]_2$ and $Cp^*RhCl(\kappa^2\text{-}OAc)$ in favor of the active species **2**. The K_{eq} value of **1** to **2** is large, and the K_{eq} value of **2** to **3** is small; therefore, **2** is formed as the major component of the equilibrium among **1**−**3** (Scheme 2). Titration of **1** with a solution of sodium acetate in methanol shows that 1 equiv of acetate converts about 50% of **1** to **2** and 2 equiv (1 mol per metal) drives the equilibrium significantly further toward **2**. Addition of 3 equiv of carboxylate strongly favors **2** over **1**. An isosbestic point is seen at 397 nm (Figure 4). Furthermore, adding 100 equiv of acetate favors the

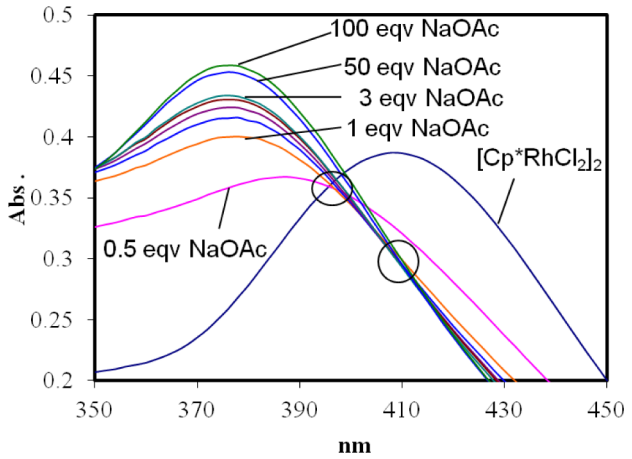

Figure 4. UV−vis study of the titration of 0.123 mM $[Cp^*RhCl_2]_2$ with excess sodium acetate in MeOH. Note two isosbestic points for **1** to **2** and for **2** to **3**.

formation of **3**. A second isosbestic point is seen at 410 nm, indicating a clean conversion of **1** → **2** → **3**. The titrations of **1** with methanol solutions of sodium difluoroacetate (Figure S3 in the Supporting Information) and sodium pivalate (Figure S4 in the Supporting Information) were studied by UV−vis as well to observe the equilibrium among dimer, monocarboxylate, and dicarboxylate. The titration with difluoroacetate shows a smooth transition from **1** to the monoacetate, and the isosbestic point is at 389 nm. A second transition is uncertain when 100 equiv of difluoroacetate was added. The titration of **1** with sodium pivalate shows the conversion to the monopivalate similarly to what is observed for acetate. The first isosbestic point is at 389 nm, and adding more than 3 equiv drives the equilibrium favorably toward the bis-pivalate, displaying an isosbestic point at 413 nm.

While only 1 equiv of acetate per metal is necessary to generate **2**, the excess carboxylate helps to buffer the carboxylic acid that is generated by the reaction. The carboxylic acid generated by CMD can also back react with the cyclometalated product if the acid is sufficiently strong, limiting the extent of reaction. These reactions typically reach 90% completion or more unless the pK_a of the conjugate acid is lower than 2.7 pK_a units (see Figure 5). The reaction with sodium difluoroacetate goes only to 60% completion after 16 h at 35 °C. Reactions with sodium cyanoacetate and sodium fluoroacetate go to ∼87% completion after 5 and 3 h, respectively, at 35 °C, and then no further change occurs, indicating the reactions have achieved equilibrium.

Effect of Carboxylate pK_a. Aryl C−H activation reactions via a base-assisted concerted metalation−deprotonation mechanism commonly use sodium acetate or sodium pivalate (NaOPiv) as a base to facilitate the deprotonation of an aromatic C−H bond.[3d,6,14] The electrophilic nature of this reaction benefits from the presence of electron-donating substituents on the arene and forms products more quickly

DOI: 10.1021/acs.organomet.5b00369
Organometallics 2015, 34, 3400−3407

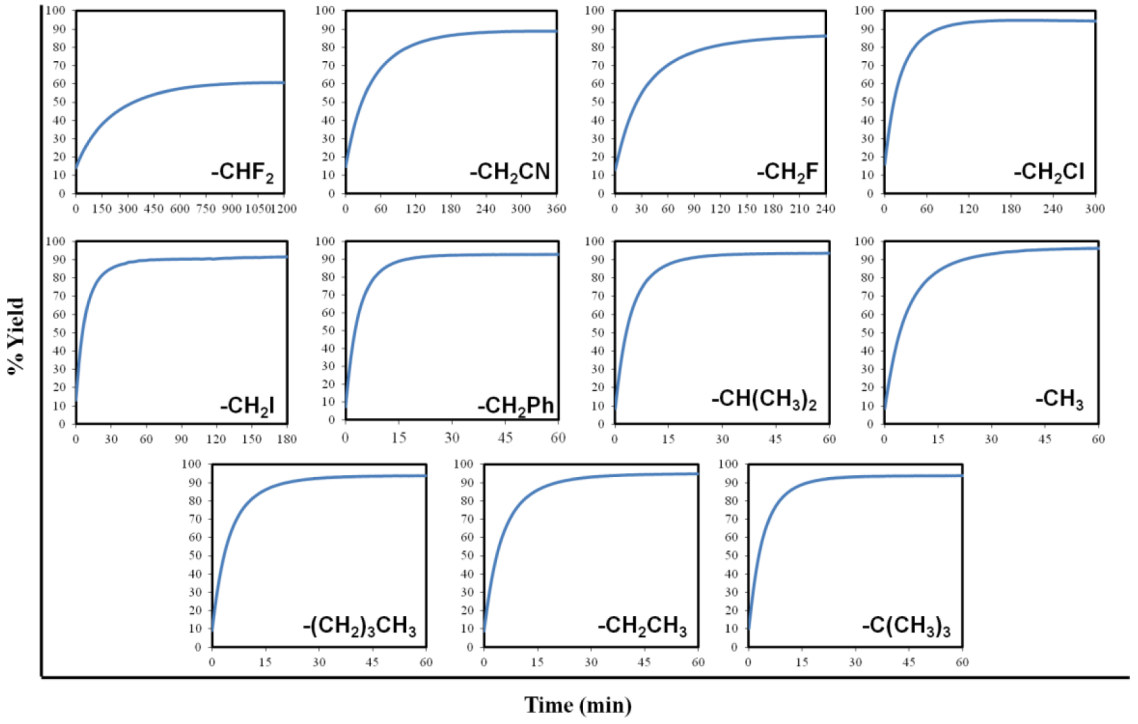

Figure 5. Kinetic plots for each carboxylate used (RCOONa). The *y* axis is time (min), and the *x* axis is observed yield. Conditions: [Rh] = [Ph′Py] = 0.627 mM; [NaOAc] = 0.934 mM; in MeOH at 35 °C.

than with less electron-rich substituents. We sought to extend this observation to the active metal species for ortho-directed aromatic C−H activation by systematically decreasing the pK_a value of the conjugate carboxylic acid. Generally, as the pK_a of the conjugate acid increases, the observed rate of reaction increases (Figure 6). The effect continues up to a pK_a value of

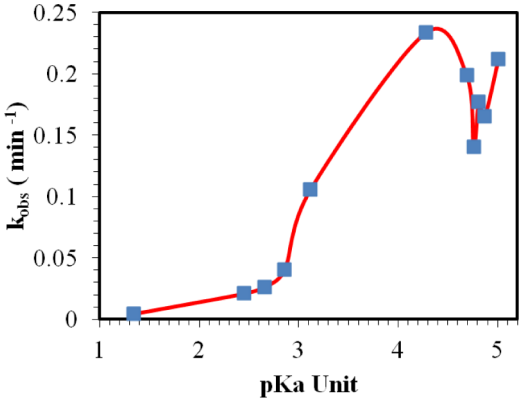

Figure 6. Observation of first-order dependence of [Ph′Py] when in excess: (red) [$Rh_{monomer}$] = 0.000314 M; (blue [$Rh_{monomer}$] = 0.000627 M.

4.3 (where sodium phenylacetate lies), and then the rate is decreased by a combination of sterics and pK_a (Table 1). The pK_a for the five carboxylates with pK_a > 4.5 span a range of only 0.3 pK_a unit. For the series methyl, ethyl, *n*-butyl, isopropyl, and *tert*-butyl the rate increases as the Taft parameter becomes larger.[15] The Taft parameter arises from a linear free energy relationship that reflects the steric influence of substituents on the rate of reaction, where the defining reaction is the acid-catalyzed hydrolysis of methyl benzoate esters. One other study was found in which the carboxylate for the concerted

Table 1. k_{obs} as a Function of Carboxylate NaO_2CR pK_a[a]

R	pK_a	Taft E_s	k_{obs}, min^{-1}
$-CHF_2$	1.34	0.67	0.00444(1)
$-CH_2CN$	2.45	0.89	0.0210(2)
$-CH_2F$	2.66	0.24	0.0265(9)
$-CH_2Cl$	2.86	0.24	0.0403(3)
$-CH_2I$	3.12	0.37	0.1057(8)
$-CH_2Ph$	4.28	0.38	0.2336(13)
$-CH(CH_3)_2$	4.69	0.47	0.1987(11)
$-CH_3$	4.76	0.0	0.1402(9)
$-(CH_2)_3CH_3$	4.81	0.31	0.1771(11)
$-CH_2CH_3$	4.87	0.07	0.1654(10)
$-C(CH_3)_3$	5.01	1.54	0.2119(11)

[a] pK_a in water.

metalation−deprotonation reaction was varied using the conjugate carboxylic acid as the solvent. The Huang group studied a C−H functionalization reaction, where they developed a selective rhodium-catalyzed C−H activation/tandem conjugate addition to α,β-unsaturated ketones under mild reaction conditions and used neat acetic acid as the solvent. As they varied the carboxylic acid solvent, they witnessed a similar effect on overall reaction yield which is consistent with our observations on the C−H cleavage step by CMD.[16]

Mechanistic Evaluation. *Concentration Effects.* In contrast with the cyclometalation reactions of benzylideneanilines with Cp*RhCl(κ²-OAc), which follow second-order kinetics,[12] all of the reactions described with Ph′Py follow clean first-order kinetics even though they are conducted under second-order conditions (1:1 metal:substrate). That is, when [Rh] = [Ph′Py], the observed rate follows eq 4 and is independent of the concentration of Ph′Py. All of the plots shown in Figure 5 show this clean first-order behavior.

DOI: 10.1021/acs.organomet.5b00369
Organometallics 2015, 34, 3400−3407

However, when Ph′Py is present in excess, the rate is first order in Ph′Py concentration, regardless of the metal concentration (Table 2, and Figure 7). These observations imply that when 1

Table 2. k_{obs} as a Function of [Ph′Py]

entry	[$Rh_{monomer}$], M	[NaOAc], M	[Ph′Py], M	k_{obs}, min^{-1}
1	0.000314	0.000467	0.00313	0.79(3)
2	0.000314	0.000467	0.00626	1.94(6)
3	0.000314	0.000467	0.00939	2.87(9)
4	0.000314	0.000467	0.0125	3.43(9)
5	0.000314	0.000467	0.0157	4.58(12)
6	0.000314	0.000467	0.0188	4.89(10)
7	0.000627	0.000934	0.000626	0.140(1)
8	0.000628	0.000934	0.00626	1.83(3)
9	0.000628	0.000934	0.0125	3.88 (12)
10	0.000628	0.000934	0.0188	6.31 (19)

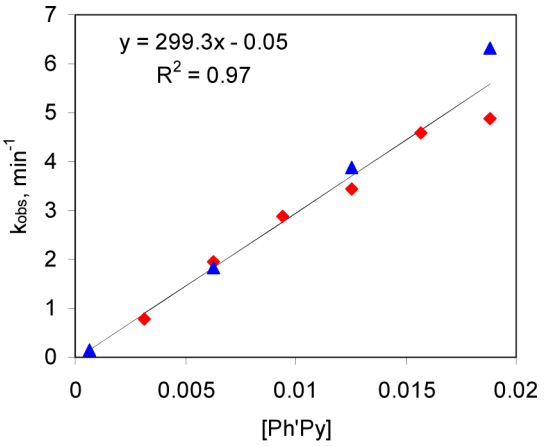

Figure 7. Observation of first-order dependence of [Ph′Py] when in excess: (red diamonds) [Rh monomer] = 0.000314 M; (blue triangles) [Rh monomer] = 0.000627 M.

equiv of substrate is present, the reaction is zero order in substrate, yet when excess Ph′Py is present, the reaction is first order in substrate. This can only be true if there is a second pathway for cyclometalation in the presense of excess substrate (vide infra).

Effect of Exogenous Bases. To determine if the observation of a first-order dependence on Ph′Py concentration can be attributed to it acting as an exogenous proton acceptor, the concentration of acetate was increased from 3 equiv per dimer up to 12 equiv per dimer. No effect on the observed rate was observed. Several different nitrogen-containing heterocycles with basicities similar to that of Ph′Py were used as additives (2-picoline, 2,6-lutidine, 4-phenylpyridine, and *N*,*N*-dimethylaminopyridine) to see how the rate would be affected. Overall the rate was unaffected when 2-picoline or 2,6-lutidine were added, but 4-phenylpyridine and DMAP showed a significant *decrease* in the rate (Figure 8). These observations are consistent with competitive binding of the nitrogen base with the Ph′Py. It is therefore unlikely that proton sequestration accelerates the observed rate when increasing the Ph′Py concentration.

Effect of Chloride Concentration. In our previous mechanistic studies with benzylideneanilines we concluded that the intermediate Cp*RhCl(κ^2-OAc) dissociates a chloride atom to generate [Cp*Rh(κ^2-OAc)]$^+$, which would then bind the benzylideneaniline.[12] Furthermore, Davies and Macgregor

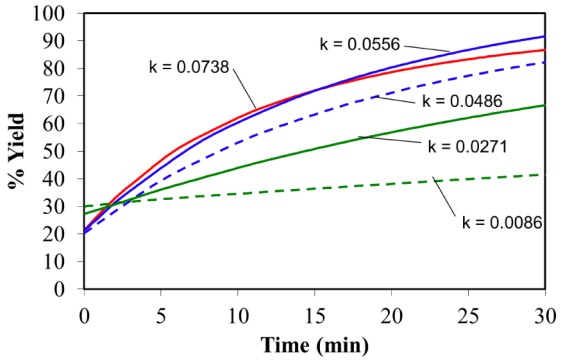

Figure 8. Plot of yield versus time with respect to added base: (red solid line) standard conditions [Rh] = [Ph′Py] = 0.314 mM and [OAc] = 0.467 mM; (blue solid line) added 0.314 mM 4-PhPy; (dashed blue line) added 0.627 mM 4-PhPy; (green solid line) added 0.314 mM DMAP; (dashed green line) added 0.627 mM DMAP. k values are given in min^{-1}.

found support for a similar intermediate metal species that is the functional C−H activation complex by DFT calculations.[11a] They found that in methanol **2** is favored over **3** and that both are favored over **1**. The complex they found as the immediate precursor to cyclometalation is [CpIr(κ^2-CO_2R) (2-PhPy)]$^+$.

Therefore, we examined [Cp*Rh(H_2O)$_3$][OTf]$_2$ in place of the neutral **1** and monitored the reaction rate (Scheme 3).

Scheme 3. Reaction of a Rh^{III} Aquo Complex with Ph′Py

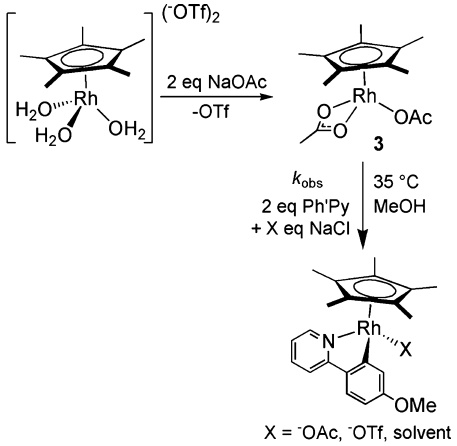

Adding sodium acetate to the rhodium−aquo complex should produce Cp*Rh(OAc)$_2$ (**3**) and change the reaction pathway, as there is no chloride present. Running the reaction of **3** with 1 equiv of Ph′Py is about 70% slower than the average observed rate for **1** (Table 3). Adding 1 equiv of NaCl nearly doubles the observed rate versus that with **1**, and adding 2 equiv of NaCl

Table 3. k_{obs} as a Function of [NaCl]

amt of NaCl/Rh, equiv	[$Rh_{monomer}$], M	[NaOAc], M	[Ph′Py], M	k_{obs}, min^{-1}
2[a]	0.000627	0.000935	0.000626	0.140(9)
0	0.000627	0.00126	0.000626	0.040(3)
1	0.000627	0.00126	0.000626	0.23(2)
2	0.000627	0.00126	0.000626	0.18(1)

[a][Cp*$RhCl_2$]$_2$ used instead of [Cp*Rh(H_2O)$_3$][OTf]$_2$.

DOI: 10.1021/acs.organomet.5b00369
Organometallics 2015, 34, 3400−3407

causes the reaction to go at a rate similar to that seen with **1** in Scheme 2, where the rhodium to chloride ratio is also 1:2.

The Davies group also investigated the ability of a triflate anion to affect the C−H activation and cleavage of DMBA-H with {CpIr$^+$} by DFT calculations. They found that triflate cleaves the dimer favorably (−9.1 kcal/mol) and forms the intermediate CpIrCl(η^1-*O*-SO_2CF_3) species, but the displacement of chloride by $\eta^1 \rightarrow \kappa^2$ conversion, coordination of DMBA-H, and C−H activation/cleavage steps are all slightly uphill from one to the next. Overall, from dimer to CpIrCl(κ^2-*C*,*N*-DMBA) plus triflic acid, the reaction is thermodynamically neutral. A reaction performed with $[Cp^*IrCl_2]_2$, DMBA-H, and sodium triflate in dichloromethane yielded very little product after 17 h, but after 4 days the reaction gave about 50% yield.[11d] This observation could suggest why the observed rate with $[Cp^*Rh(H_2O)_3][OTf]_2$ is slow in the absence of chloride on the basis of the favorable coordination of the triflate anion, which could bind competitively, but is an ineffective base for CMD. Recent DFT calculations also indicate that coordination of chloride drives the reaction thermodynamically.[11a]

Mechanistic Proposal. Scheme 4 shows a proposed mechanism that is consistent with the experimental observations. **1**−**3** are all in equilibrium with a large K_{eq} value favoring the Cp*RhCl(κ^2-OAc) species and a small K_{eq} value for forming $Cp^*Rh(OAc)_2$. Either **2** or **3** can go on to the key intermediate Cp*Rh$^+$(κ^2-OAc) (**A**), by losing either chloride or acetate, respectively. Once **A** is generated, it would immediately coordinate Ph′Py to make **B**. In our previous study with benzylideneanilines the rate of dissociation of chloride to generate **A** was comparable to the rate of the C−H activation step owing to the poor Lewis basicity of the imine, requiring formation of a poorly stabilized intermediate prior to C−H activation. DFT calculations of the imine activation by Davies and Macgregor also support that formation of the N-bound adduct is uphill thermodynamically.[11a] In the present case, the C−H activation step is also rate limiting but the Ph′Py can coordinate easily to the rhodium center once the acetate has been attached. DFT calculations by Davies and Macgregor also support that coordination of phenylpyridine is downhill for rhodium from the dimer and slightly uphill from Cp*Rh(OAc)Cl (1 kcal/mol).[11a] With 4-methoxyphenylpyridine, the binding is expected to be even stronger.

Scheme 4. Proposed Mechanistic Pathway

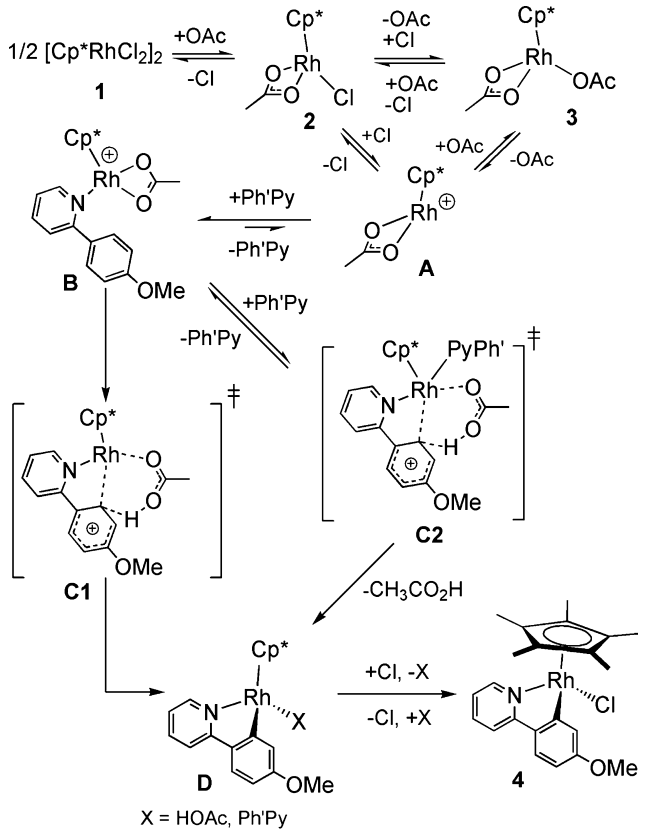

In support of this hypothesis an independently synthesized solution of Cp*RhCl(κ^2-OAc) in CD_3OD was mixed with 1 equiv of 4-picoline at room temperature in an NMR tube. Within the time it took to add the 4-picoline to the solution of Cp*RhCl(κ^2-OAc) and mix, all of the 4-picoline had coordinated to the rhodium (Figure 9), giving [Cp*Rh(κ^2-OAc)(4-picoline)]$^+$. Also, in another experiment, $Cp^*Rh(OAc)_2$ was synthesized and evaluated by ^{1}H NMR spectroscopy in deuterated methanol.[17] There is a major peak at δ 1.53 for Cp* that is not seen in the experiment described with **1**, sodium acetate, and 4-picoline in deuterated methanol, where the Cp* peak is about δ 1.58. However, what is observed is a peak at δ 1.66 which vanishes after 4-picoline is added and is likely to be a coordinated water molecule.[17]

B is set up for concerted metalation−deprotonation to occur with assistance from the acetate via transition state **C1**. This creates **D** with a weakly coordinating group such as carboxylic acid, solvent, or another molecule of Ph′Py. In the case with excess Ph′Py, binding a second Ph′Py could lead to a reaction with acetate via transition state **C2** to give product **4** at a rate faster than that via **C1**, thereby accounting for the first-order dependence observed when excess Ph′Py is present.

In support of the hypothesis of a second weakly coordinating Ph′Py ligand, Ellman has recently isolated and reported a complex similar to **D** (X = 2-PhPy), [Cp*Rh(κ^2-C,N-PhPy)(κ^1-*N*-PhPy)]$^+$, from a reaction of **1** with 4 equiv of $AgSbF_6$ and 6 equiv of 2-phenylpyridine.[8b] The reaction also generated pyridinium salt, suggesting the excess 2-phenylpyridine acted as the deprotonation assistant in a concerted metalation−deprotonation fashion. The cyclometalated species displayed broad resonances by ^{1}H NMR spectroscopy, and decomposition began after a few hours at room temperature in dichloromethane.

In the presence of excess 2-phenylpyridine, however, the complex was stable.[8b] The [Cp*Rh(κ^2-*C*,*N*-PhPy)(κ^1-*N*-PhPy)]$^+$ complex was shown to be a catalyst resting state in the C−H arylation of imines, where once the [Cp*Rh(κ^2-*C*,*N*-PhPy)(η^1-*N*-PhPy)]$^+$ complex formed, the loss of η^1-*N*-PhPy was necessary to generate the 16-electron intermediate that could then bind imine substrate to continue in the catalytic cycle.

CONCLUSION

The effect of the carboxylate used in a concerted metalation−deprotonation reaction has been studied and has shown a direct correlation of pK_a to observed rate up to a pK_a of 4.3, where the rate drops off at higher pK_a. The rate of the C−H activation of 2-(4-methoxyphenyl)pyridine with $[Cp^*RhCl_2]_2$ and carboxylate follows first-order kinetics in the active metal species, Cp*RhCl(κ^2-OAc), and zero-order kinetics in substrate when in a 1:1 ratio. There was a first-order dependence on substrate observed when excess substrate is present. This suggests that,

DOI: 10.1021/acs.organomet.5b00369
Organometallics 2015, 34, 3400−3407

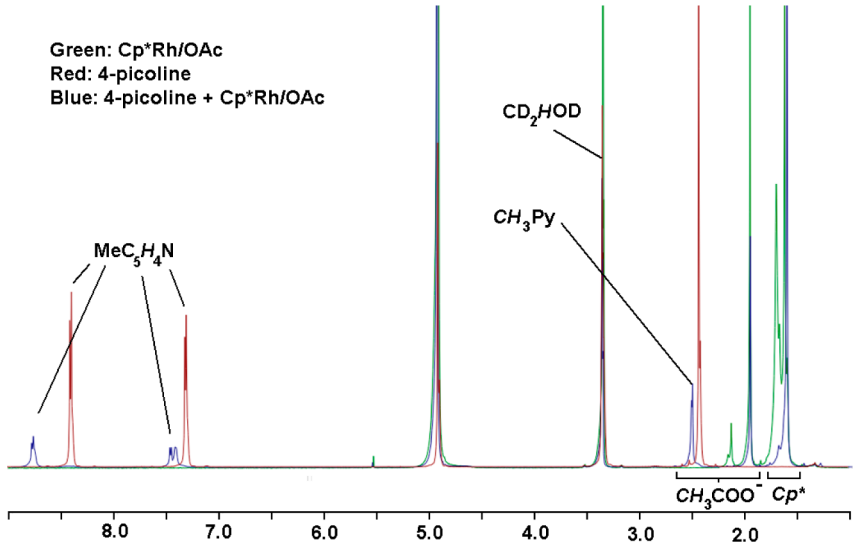

Figure 9. NMR experiment of Cp*RhCl(κ^2-OAc) and 4-picoline (1:1) before and after mixing at room temperature.

while studying the kinetics of the reaction under stoichiometric conditions provides useful information, it does not necessarily mean that the reaction follows those observed kinetics under catalytically relevant conditions. The evalution of the mechanism using kinetic studies allowed for a mechanistic proposal in which a second Ph′Py coordinates prior to the rate-determining C−H activation.

EXPERIMENTAL SECTION

General Procedures, Materials, and Instrumentation. $RhCl_3 \cdot 3H_2O$ was purchased from Pressure Chemical Co., and $[Cp^*RhCl_2]_2$ was prepared according to the literature.[18] Chloroacetic acid, phenylacetic acid, pivalic acid, sodium iodoacetate, sodium acetate, sodium trifluoroacetate and sodium *tert*-butoxide (2 M in THF) were purchased from Sigma-Aldrich. Cyanoacetic acid, difluoroacetic acid, 2-(4-methoxyphenyl)pyridine, methyl fluoroacetate, and 2-phenylpyridine were purchased from TCI Chemicals. Isobutyric acid and valeric acid were purchased from Acros Organics. Sodium hydroxide and methanol were purchased from Fisher Scientific. 4-Picoline was purchased from Alfa Aesar. Propionic acid was purchased from Eastman Kodak. Sodium carbonate was purchased from Macron Chemicals. All purchased materials were used as received. Tetrahydrofuran, diethyl ether, and dichloromethane were purchased from Fisher Scientific and purified by passage through activated alumina columns in an Innovative Technology, Inc., PS-MD-6 solvent purification system. Deuterated solvents were purchased from Cambridge Isotope Laboratories. Chloroform-d_1 (δ 7.26) was used as received, and methanol-d_4 (δ 3.31) was dried over 4 Å molecular sieves (activated under vacuum while heating overnight) and distilled under vacuum. ^{1}H NMR spectra were recorded using an Avance 400 MHz spectrometer, and $^{13}C\{^1H\}$ NMR spectra were recorded using an Avance 500 MHz spectrometer. UV−vis kinetics were carried out using a Hewlett-Packard 8452 diode array spectrophotometer with a Hewlett-Packard 89090A Peltier temperature controller. Elemental analyses were determined by the CENTC Elemental Analysis Facility at the University of Rochester using a PerkinElmer 2400 SeriesII analyzer equipped with a PerkinElmer Model AD-6 autobalance by Dr. William W. Brennessel. IR spectra were recorded using a Shimadzu IR Prestige-21 FTIR spectrophotometer with a PIKE Technologies MIRacle single-reflection ATR. X-ray diffraction data were collected using a Bruker SMART APEX II CCD Platform diffractometer.

Synthesis of Cp*RhCl(2-(4-methoxyphenyl)pyridine) (4). The synthesis was analogous to the previously published procedure.[13] The crude material was crystallized via vapor diffusion of cyclohexane into a saturated CH_2Cl_2 solution; purified yield 39.7 mg (80%). ^{1}H NMR (400 MHz, $CDCl_3$): δ 8.65 (d, J = 5.2 Hz, 1H), 7.62 (m, 2H), 7.53 (d, J = 8.4 Hz, 1H), 7.36 (d, J = 2 Hz, 1H), 7.03 (dt, J = 5.8, 1.6 Hz, 1H), 6.61 (dd, J = 8.4, 2 Hz, 1H), 3.9 (s, 3H), 1.62 (s 15H). $^{13}C\{^1H\}$ NMR (125 MHz, $CDCl_3$): δ 180.9, 180.6, 165.3, 160.6, 151.2, 137.0 (d), 121.3, 120.9, 118.4, 109.4, 96.0 (d), 55.2, 9.3. Anal. Calcd (found) for $C_{22}H_{25}ClNORh$: C, 57.72 (57.81); H, 5.504 (5.40); N, 3.06 (3.04).

Synthesis of Sodium Difluoroacetate. Sodium carbonate (562.7 mg, 5.3 mmol) was placed in a round-bottom flask followed by a stir bar and 10 mL of THF. Difluoroacetic acid (0.67 mL, 10.6 mmol) was added with stirring, and then a reflux condenser was attached and the flask was submerged in an oil bath and refluxed for 3 h. The reaction mixture was cooled and filtered through a frit while warm to give a white solid, that was dried under vacuum overnight; yield 1.21 g (97%). IR (solid): 1634 cm^{-1} (C═O). Mp: 172−174 °C. Anal. Calcd (found) for $C_2HF_2NaO_2$: C, 20.35 (20.25); H, 0.85 (0.78).

Synthesis of Sodium Cyanoacetate. Cyanoacetic acid (372.4 mg, 4.3 mmol) was placed in a round-bottom flask followed by a stir bar and 10 mL of THF. The flask was sealed with a septum, the solution was stirred, and the flask was submerged in an ice−water bath. Then sodium *tert*-butoxide (2.16 mL, 4.3 mmol) was added to the mixture, dropwise, over the course of 10 min. Instant precipitation of a white solid occurred, and the mixture was stirred for 2 h. The mixture was then filtered through a frit and washed with three portions of cold diethyl ether (25 mL total). The solid was dried under high vacuum overnight; yield 400.4 mg (99%). IR (solid): 2256 cm^{-1} (C≡N), 1598 cm^{-1} (C═O). Mp: 175−176 °C. Anal. Calcd (found) for $C_3H_2NaNO_2$: C, 33.66 (33.55); H, 1.88 (1.95); N, 13.08 (12.72).

Synthesis of Sodium Fluoroacetate. Ground sodium hydroxide (399.5 mg, 10 mmol) was placed in a round-bottom flask followed by a stir bar and 10 mL of THF. Methyl fluoroacetate (0.78 mL, 10 mmol) was then added, a reflux condenser was attached, and the flask was submerged in an oil bath and refluxed for 2 h with stirring. The mixture was cooled to room temperature, and the solvent was evaporated to give a white solid which was dried under high vacuum overnight; yield 946.1 mg (94%). IR (solid): 1608 cm^{-1} (C═O). Mp: >170 °C dec. Anal. Calcd (found) for $C_2H_2FNaO_2$: C, 24.01 (23.87); H, 2.015 (1.97).

Synthesis of Sodium Chloroacetate. The synthesis is analogous to NaO_2CCH_2CN; yield 99%. IR (neat): 1591 cm^{-1} (C═O). Mp: >170 °C dec. Anal. Calcd (found) for $C_2H_2ClNaO_2$: C, 20.62 (20.24); H, 1.73 (1.65).

Synthesis of Sodium Phenylacetate. Sodium carbonate (75.6 mg, 0.713 mmol) was placed in a round-bottom flask followed by a stir bar. Then phenylacetic acid (194.7 mg, 1.43 mmol) was added, followed by 5 mL of distilled water, and the solution was stirred vigorously for 30 min. The solvent was evaporated and the solid white

DOI: 10.1021/acs.organomet.5b00369
Organometallics 2015, 34, 3400−3407

residue washed onto a frit with THF. The residue was dried under high vacuum overnight; yield 143.4 mg (63%). IR (solid): 1569 cm^{-1} (C═O). Mp: 182−184 °C. Anal. Calcd (found) for $C_8H_7NaO_2$: C, 60.76 (60.31); H, 4.46 (4.59).

Synthesis of Sodium Isobutyrate. The synthesis is analogous to NaO_2CH_2Ph; yield 212.7 mg (75%). IR (solid): 1549 cm^{-1} (C═O). Mp: > 250 °C. Anal. Calcd (found) for $C_4H_7NaO_2$: C, 43.64 (43.69); H, 6.41 (6.13).

Synthesis of Sodium Valerate. The synthesis was analogous to NaO_2CCH_2CN; yield 314 mg (86%). IR (neat): 1552 cm^{-1} (C═O). Mp: 238 °C. dec. Anal. Calcd (found) for $C_5H_9NaO_2$: C, 48.38 (48.11); H, 7.31 (7.17).

Synthesis of Sodium Propanoate. The synthesis was analogous to NaO_2CCH_2CN; yield 258.9 mg (89%). IR (solid): 1557 cm^{-1} (C═O). Mp: 288−290 °C. Anal. Calcd (found) for $C_3H_5NaO_2$: C, 37.51 (37.68); H, 5.16 (4.73).

Synthesis of Sodium Pivalate. The synthesis is analogous to NaO_2CH_2Ph; yield 400.5 mg (80%). IR (solid): 1549 cm^{-1} (C═O). Mp: > 400 °C. Anal. Calcd (found) for $C_5H_9NaO_2$: C, 48.39 (48.18); H, 7.31 (7.05).

General Procedures for Kinetic Experiments: UV−Vis Protocol. Each volumetric flask was dried in an oven overnight and cooled under nitrogen before use. A 14.5 mg portion of **1** (0.023 mmol) was dissolved in 25 mL of methanol. A 34.6 mg portion of Ph′Py (0.186 mmol) was dissolved in 25 mL of methanol. For each carboxylate 0.056 mmol was dissolved in 5 mL of methanol.

For a typical reaction 100 μL of a 9.41 × 10^{-4} M solution of $[Cp^*RhCl_2]_2$ in methanol was placed in a 1 mm path length quartz cuvette with 150 μL of methanol. The cuvette was sealed and inverted five times, and the spectrum was recorded. Then 25 μL of a 1.12 × 10^{-2} M solution of the carboxylate in methanol was placed in the cuvette. The cuvette was sealed and inverted five times, and the spectrum was recorded. Finally, 25 μL of a 7.53 × 10^{-3} M solution of 2-(4-methoxyphenyl)pyridine in methanol was placed in the cuvette. The cuvette was sealed and inverted once, and the experiment was started while wavelength was monitored at 338 nm with the cuvette-holder temperature set to 35 °C. The length of the experiment and the number of spectra recorded varied depending on the carboxylate used.

■ ASSOCIATED CONTENT

Ⓢ Supporting Information

Figures, tables, and a CIF file giving crystallographic data and additional experimental data. The Supporting Information is available free of charge on the ACS Publications website at DOI: 10.1021/acs.organomet.5b00369. X-ray structural data have also been deposited with the Cambridge Crystallographic Data Centre (CCDC deposition #1060122).

■ AUTHOR INFORMATION

Corresponding Author

*E-mail for W.D.J.: jones@chem.rochester.edu.

Notes

The authors declare no competing financial interest.

■ ACKNOWLEDGMENTS

This work has been supported by the National Science Foundation, grant CHE-1360985. The authors also thank William W. Brennessel for carrying out the X-ray crystal structure determination of **3** and performing elemental analyses via the CENTC Elemental Analysis Facility (CHE-0650456).

■ REFERENCES

(1) (a) Blanksby, S. J.; Ellison, G. B. *Acc. Chem. Res.* **2003**, *36*, 255. (b) Bordwell, F. G. *Acc. Chem. Res.* **1988**, *21*, 456.

(2) Kuhl, N.; Hopkinson, M. N.; Wencel-Delord, J.; Glorius, F. *Angew. Chem., Int. Ed.* **2012**, *51*, 10236.

(3) Issue 7, volume 356, of *Advanced Synthesis and Catalysis* is a special issue devoted to directed C−H functionalization. (a) Giri, R.; Thapa, S.; Kafle, A. *Adv. Synth. Catal.* **2014**, *356*, 1395. (b) Shi, G.; Zhang, Y. *Adv. Synth. Catal.* **2014**, *356*, 1419. (c) Kuhl, N.; Schröder, N.; Glorius, F. *Adv. Synth. Catal.* **2014**, *356*, 1443. (d) De Sarkar, S.; Liu, W.; Kozhushkov, S. I.; Ackermann, L. *Adv. Synth. Catal.* **2014**, *356*, 1461.

(4) (a) Zhang, M.; Zhang, Y.; Jie, X.; Zhao, H.; Li, G.; Su, W. *Org. Chem. Front.* **2014**, *1*, 843. (b) Rouquet, G.; Chatani, N. *Angew. Chem., Int. Ed.* **2013**, *52*, 11726.

(5) Han, Y.; Jin, G. *Chem. Soc. Rev.* **2014**, *43*, 2799.

(6) Kapdi, A. R. *Dalton Trans.* **2014**, *43*, 3021. Ackermann, L. *Chem. Rev.* **2011**, *111*, 1315.

(7) (a) LaPointe, D.; Fagnou, K. *Chem. Lett.* **2010**, *39*, 1118. (b) Fagnou, K. *Top. Curr. Chem.* **2010**, *292*, 35. (c) Guimond, N.; Gouliaras, C.; Fagnou, K. *J. Am. Chem. Soc.* **2010**, *132*, 6908.

(8) (a) Colby, D. A.; Tsai, A. S.; Bergman, R. S.; Ellman, J. A. *Acc. Chem. Res.* **2012**, *45*, 814. (b) Tsai, A. S.; Tauchert, M. E.; Bergman, R. G.; Ellman, J. A. *J. Am. Chem. Soc.* **2011**, *133*, 1248. (c) Hesp, K. D.; Bergman, R. G.; Ellman, J. A. *Org. Lett.* **2012**, *14*, 2304. (d) Tauchert, M. E.; Incarvito, C. D.; Rheingold, A. L.; Bergman, R. G.; Ellman, J. A. *J. Am. Chem. Soc.* **2012**, *134*, 1482. (d) Wangweerawong, A.; Bergman, R. G.; Ellman, J. A. *J. Am. Chem. Soc.* **2014**, *136*, 8520.

(9) (a) Ackermann, L. *Acc. Chem. Res.* **2014**, *47*, 281. (b) Ackermann, A.; Vicente, R.; Althammer, L. *Org. Lett.* **2008**, *10*, 2299. (c) Ackermann, L.; Potukuchi, H. K.; Vicente, R.; Pirovano, V. *Org. Lett.* **2010**, *12*, 5032.

(10) Pfeffer, M. *Pure Appl. Chem.* **1992**, *64*, 335.

(11) (a) Carr, K. J. T.; Davies, D. L.; Macgregor, S. A.; Singh, K.; Villa-Marcos, B. *Chem. Sci.* **2014**, *5*, 2340. (b) Boutadla, Y.; Davies, D. L.; Jones, R. C.; Singh, K. *Chem. - Eur. J.* **2011**, *17*, 3438. (c) Boutadla, Y.; Al-Duaij, O.; Davies, D. L.; Griffith, G. A.; Singh, K. *Organometallics* **2009**, *28*, 433. (d) Boutadla, Y.; Davies, D. L.; Macgregor, S. A.; Poblador-Bahamonde, A. I. *Dalton Trans.* **2009**, *38*, 5887. (e) Davies, D. L.; Donald, S. M. A.; Al-Duaij, O.; Macgregor, S. A.; Pölleth, M. *J. Am. Chem. Soc.* **2006**, *128*, 4210. (f) Davies, D. L.; Donald, S. M. A.; Macgregor, S. A. *J. Am. Chem. Soc.* **2005**, *127*, 13754. (g) Davies, D. L.; Al-Duaij, O.; Fawcett, J.; Giardiello, M.; Hilton, S. T.; Russell, D. R. *Dalton Trans.* **2003**, *21*, 4132.

(12) Li, L.; Brennessel, W. W.; Jones, W. D. *Organometallics* **2009**, *28*, 3492.

(13) Li, L.; Brennessel, W. W.; Jones, W. D. *J. Am. Chem. Soc.* **2008**, *130*, 12414.

(14) Arockiam, P. B.; Bruneau, C.; Dixneuf, P. H. *Chem. Rev.* **2012**, *112*, 5879.

(15) (a) Taft, R. W. *J. Am. Chem. Soc.* **1953**, *75*, 4538. (b) Taft, R. W. *J. Am. Chem. Soc.* **1952**, *74*, 3120. (c) Taft, R. W. *J. Am. Chem. Soc.* **1952**, *74*, 2729.

(16) Yang, L.; Qian, B.; Huang, H. *Chem. - Eur. J.* **2012**, *18*, 9511.

(17) Boyer, P. M.; Roy, C. P.; Bielski, J. M.; Merola, J. S. *Inorg. Chim. Acta* **1996**, *245*, 7.

(18) Kang, J. W.; Moseley, K.; Maitlis, P. M. *J. Am. Chem. Soc.* **1969**, *91*, 5970.

DOI: 10.1021/acs.organomet.5b00369
Organometallics 2015, 34, 3400−3407